Spatiotemporal Dynamics of Memory Encoding and Memory Retrieval States

Yuju Hong, Isabelle L. Moore, Devyn E. Smith, and Nicole M. Long

Abstract

■ Memory encoding and memory retrieval are neurally distinct brain states that can be differentiated on the basis of cortical network activity. However, it is unclear whether sustained engagement of one network or fluctuations between multiple networks give rise to these memory states. The spatiotemporal dynamics of memory states may have important implications for memory behavior and cognition; however, measuring temporally resolved signals of cortical networks poses a challenge. Here, we recorded scalp electroencephalography from participants performing a mnemonic state task in which they were biased toward memory encoding or retrieval. We performed a microstate analysis to measure the temporal dynamics of cortical networks throughout this mnemonic state task. We find that Microstate E, a putative analog of the default mode network, shows temporally sustained dissociations between memory encoding and retrieval, with greater engagement during retrieve compared with encode trials. We further show that decreased engagement of Microstate E is a general property of encoding, rather than a reflection of retrieval suppression. Thus, memory success, as well as cognition more broadly, may be influenced by the ability to engage or disengage Microstate E in a goal-dependent manner. ■

INTRODUCTION

Successful memory depends on both the formation of a representation of a new experience—encoding—and subsequently accessing the stored representation of a past experience—retrieval. Although brain activity patterns during encoding are commonly reinstated during retrieval (Ritchey, Wing, LaBar, & Cabeza, 2013; Polyn, Natu, Cohen, & Norman, 2005; Wheeler, Petersen, & Buckner, 2000), there is growing evidence that memory encoding and retrieval constitute distinct brain states (Richter, Chanales, & Kuhl, 2016; Hasselmo, 2005) supported by cortical network activity (Long & Kuhl, 2021). However, it is unclear whether memory states are supported by the sustained engagement of a specific network or rapid fluctuations between distinct networks. Memory states influence processing and behavior (Smith, Moore, & Long, 2022; Long & Kuhl, 2021, 2019); encoding and retrieval failures may be because of over- or underreliance on one or more cortical networks. The aim of this study is to investigate the spatiotemporal dynamics of memory states.

Attention, control, memory, and other cognitive demands recruit distinct resting-state networks (RSNs). Identified via resting-state fMRI, RSNs reflect nodes of the cortex whose activity is intrinsically correlated (Power et al., 2011; Yeo et al., 2011; Fox et al., 2005). RSNs show both sustained and transient activity fluctuations in response to task demands. The ventral attention (VAN) and frontoparietal control (FPCN) networks are engaged at different moments in time during decision-making tasks (Gratton et al., 2016) as are the default mode network (DMN) and the dorsal attention network (DAN) during arithmetic tasks (Raccah, Daitch, Kucyi, & Parvizi, 2018). The DMN, commonly "deactivated" during cognitive tasks (Raichle et al., 2001), is engaged during episodic memory retrieval (Kim, 2010), semantic processing (Binder, Desai, Graves, & Conant, 2009), and internally directed attention (Buckner & DiNicola, 2019). There is likewise evidence that communication between RSNs supports cognitive processing, in particular that connectivity between the FPCN and the DMN supports internally directed attention (Kam et al., 2019), and other forms of internal mentation, including working memory (Murphy, Bertolero, Papadopoulos, Lydon-Staley, & Bassett, 2020) and memory search (Kragel & Polyn, 2013). Together, these findings broadly point to a role for RSNs in cognition, but leave open the question of how the temporal dynamics of RSNs support memory states.

Encoding and retrieval states can be distinguished via multivariate pattern classification analysis of cortical signals. Although there exist multiple definitions of "brain state" ("unique configuration of anatomy, physiology, representation and behavior," Kay & Frank, 2019; "recurring patterns of correlation between networks," Beaty et al., 2018; "the reliable patterns of brain activity that involve the activation and/or connectivity of multiple large-scale brain networks," Tang, Rothbart, & Posner, 2012), the general theme across these definitions is that brain states are

University of Virginia, Charlottesville

inherently multivariate in nature. That is, a single brain region, neuronal population, and/or electrical signal is unlikely to be the sole substrate responsible for a particular brain state. Consistent with the interpretation that encoding and retrieval reflect brain states, we have found that encoding and retrieval recruit distinct whole-brain activity patterns. Spectral activity across electrodes placed on the scalp (Smith et al., 2022; Long & Kuhl, 2019) as well as fMRI BOLD activity across cortical regions and networks (Long & Kuhl, 2021; Richter et al., 2016) differentiate encoding from retrieval states.

Despite evidence that encoding and retrieval states are neurally dissociable, it is unclear whether memory states are supported by sustained or transient engagement of RSNs. Identifying the temporal dynamics of memory states is important because it will provide insights into how these states are selectively engaged or disengaged. Although multivariate pattern classifiers can distinguish states based on cortical activity patterns, such dissociations may be driven by rapid shifts between multiple networks rather than sustained engagement of an individual network. As classifier feature weights reveal the substrates that contribute to classification performance, as opposed to all substrates that dissociate the conditions of interest, investigation of classifier features is necessarily limited (Haufe et al., 2014). Similarly, whereas univariate investigation of voltage and/or spectral signals will reveal specific substrates (e.g. electrode/frequency combinations) that dissociate memory states, such approaches are not suitable for identifying the whole-brain network configurations that underlie memory states. Therefore, to identify the temporal dynamics that underlie memory states, it is necessary to adopt an analytical approach that yields time-resolved signals from cortical networks.

Temporal dynamics of RSNs can be measured through the investigation of *microstates* (Lehmann, Ozaki, & Pal, 1987). Microstates are global patterns of voltage scalp topographies that remain stable for a sustained period (approximately 60–120 msec; Michel & Koenig, 2018). Four canonical microstates (A, B, C, and D) have been identified across both resting and task-based studies, although there is evidence for additional microstates (E, F, G, and subdivisions of C) beyond the canonical four. Unlike traditional investigations of scalp EEG signals, microstates are reference-independent (Brunet, Murray, & Michel, 2011) and inherently multivariate, capturing whole-brain dynamics rather than relying on electrode-by-electrode signal comparisons (Tzovara, Murray, Michel, & De Lucia, 2012). Microstates may represent basic building blocks of cognition (Seitzman et al., 2017), and as a topographic measure, microstates reflect the configuration of brain sources (Tzovara et al., 2012).

Studies employing simultaneous EEG and fMRI recordings, as well as source-localization methods, indicate that EEG microstates are closely associated with fMRI RSNs, including the visual, attention, and DMN (Michel & Koenig, 2018; Custo et al., 2017; Yuan, Zotev, Phillips, Drevets, & Bodurka, 2012; Britz, Van De Ville, & Michel, 2010). For instance, Microstate B shows increased engagement during eyes-open compared with eyes-closed rest (Seitzman et al., 2017) and is linked with the visual network (Britz, Van De Ville, & Michel, 2010). Microstate D, thought to reflect the DAN (Britz et al., 2010), is engaged during a serial subtraction task (Seitzman et al., 2017) and processes that (re)orient attention (Milz et al., 2016). Finally, both Microstates C and E have been linked with the DMN (Bréchet et al., 2019; Custo et al., 2017) and show increased engagement during eyes-closed rest, memory retrieval, and mind wandering (Bréchet et al., 2019; Koenig et al., 2002). Microstate C has also been associated with the saliency network or VAN (Britz et al., 2010). Thus, as microstates enable measurement of large-scale cognitive networks (Khanna, Pascual-Leone, & Farzan, 2014), they provide the ideal method for assessing the spatiotemporal dynamics of memory brain states.

Our hypothesis is that memory brain states are supported by distinct patterns of cortical topography or microstates that are sustained over time. The alternative is that fluctuations between multiple different microstates give rise to encoding and retrieval states. To test our hypothesis, we recorded scalp EEG while participants engaged in a mnemonic state task (Smith et al., 2022). Briefly, participants were instructed to either encode the currently presented stimulus or to retrieve a previously presented, related stimulus. These instructions were intended to bias participants toward either an encoding or retrieval state. Using established methods (Murray, Brunet, & Michel, 2008), we measured microstate engagement over time as participants were biased toward these memory states.

METHODS

Participants

One hundred nine (65 women, age range = 18–66 years, mean age = 21.64 years) fluent English speakers from the University of Virginia community participated. All participants had normal or corrected-to-normal vision. Informed consent was obtained in accordance with the University of Virginia Institutional Review Board for Social and Behavioral Research, and participants were compensated for their participation. As the current study was conducted in tandem with multiple other studies from our laboratory, sample size for this specific investigation was not determined a priori. Instead, we used a sample size of $n = 40$ for the primary studies, based on prior work, and then aggregated the data in this task across all of the primary studies. Not all participants in the primary study chose to perform this task. Ten participants were excluded from the final data set: One had previously participated in a behavioral version of the experiment, one had poor EEG signal quality, two failed to comply with task instructions, two had corrupt data files, and four did not have any

resting-state data. Thus, the reported data are from the remaining 99 participants. A subset of this data set was previously reported (Smith et al., 2022); all of the analyses and results described here are novel. The raw, de-identified data and the associated experimental and analysis codes used in this study can be accessed via the Long Term Memory laboratory website (https://longtermmemorylab.com).

Mnemonic State Task Experimental Design

Stimuli consisted of 576 object pictures, drawn from an image database with multiple exemplars per object category (Konkle, Brady, Alvarez, & Oliva, 2010). From this database, we chose between 108 and 216 unique object categories and two exemplars from each category. For each participant, one exemplar served as a List 1 object and one as a List 2 object; object condition assignment was randomly generated for each participant.

General Overview

Participants completed between 6 and 12 runs in which they viewed two lists containing 18 object images. For the first list, each object was new (List 1 objects). For the second list (List 2 objects), each object was again new, but was categorically related to an object from the first list. For example, if List 1 contained an image of a bench, List 2 would contain an image of a different bench (Figure 1). During List 1, participants were instructed to encode each new object. During List 2, each trial contained an instruction to either encode the current object (e.g., the new bench) or to retrieve the corresponding object from List 1 (the old bench). Following the study phase, participants completed a recognition phase that tested participants' memory of List 1 and List 2 objects. Because subsets of participants completed different types of recognition memory tests (n = 45 two alternative forced-choice test; n = 52 recency test) or did not complete a memory test (n = 2), we do not report the memory test data here.

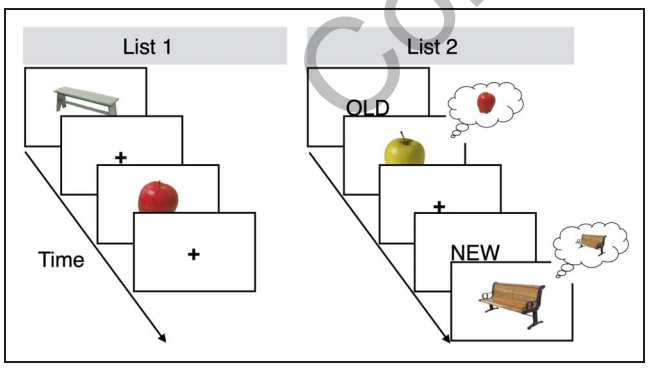

Figure 1. Mnemonic state task design. During List 1, participants studied individual objects (e.g., bench, apple) for 2000 msec followed by a 1000-msec ISI. During List 2, participants saw novel objects that were from the same categories as the objects shown in List 1 (e.g., a new bench, a new apple). Preceding each List 2 object was an "OLD" instruction cue or "NEW" instruction cue. The "OLD" cue signaled that participants were to retrieve the corresponding object from List 1 (e.g., the old bench). The "NEW" cue signaled that participants were to encode the current object (e.g., the new apple). Each run of the experiment contained a List 1 and List 2; object categories (e.g., bench) were not repeated across runs.

List 1

On each trial, participants saw a single object presented for 2000 msec followed by a 1000-msec ISI. Participants were instructed to study the presented object in anticipation of a later memory test.

List 2

On each trial, participants saw a cue word, either "OLD" or "NEW" for 2000 msec. The cue was followed by a presentation of an object for 2000 msec, which was followed by a 1000-msec ISI. All objects in List 2 were non-identical exemplars drawn from the same category as the objects presented in the immediately preceding List 1 of the same run. That is, if a participant saw a bench and an apple during List 1, a different bench and a different apple would be presented during List 2. On trials with a NEW instruction (encode trials), participants were to encode the presented object. On trials with an OLD instruction (retrieve trials), participants tried to retrieve the categorically related object from the preceding List 1. Importantly, this design prevented participants from completely ignoring List 2 objects following OLD instructions in that they could only identify the to-be-retrieved object category by processing the List 2 object.

Participants completed 6–12 runs with two lists in each run (List 1 and List 2). Participants viewed 18 objects per list, yielding 216–288 object stimuli from 108 to 216 unique object categories. Participants did not make a behavioral response during either List 1 or List 2.

Resting-State Task

After the mnemonic state task, the participants completed a simple and cognitively nondemanding resting-state task. The task consisted of eight runs with 10 trials per run. During each trial, participants viewed five asterisks presented on a computer screen, with one asterisk at the center of the screen and the four others at the top, bottom, left, and right sides of the screen relative to the center. Participants performed one of four types of eye movements during each run, with the specific type indicated by an auditory cue. During open/close runs, participants were instructed to open or close their eyes. During left/right runs, participants were instructed to saccade to the left or right asterisk. During up/down runs, participants were instructed to saccade to the top or bottom asterisk. During the blink runs, participants were instructed to blink following the auditory cue. All auditory cues within a run were separated by an ISI. For 41

participants, the ISI was a fixed interval of 5000 msec. For 58 participants, the ISI could vary randomly between 3000 msec and 9000 msec with an average of 6500 msec. For all runs except blink runs, the auditory cues alternated (e.g., "open," "close," "open," "close") and were evenly divided into five of each subtype. We only utilized the open/close runs and omitted all other runs from our analyses.

EEG Data Acquisition and Preprocessing

EEG recordings were collected using a BrainVision system and an ActiCap equipped with 64 Ag/AgCl active electrodes positioned according to the extended 10–20 system. All electrodes were digitized at a sampling rate of 1000 Hz and were referenced to electrode FCz. Offline, electrodes were later converted to an average reference. Impedances of all electrodes were kept below 50 kΩ. Electrodes that demonstrated high impedance or poor contact with the scalp were excluded from the average reference; however, these electrodes were included in all subsequent analysis steps. Bad electrodes were determined by voltage thresholding (see below).

Custom Python codes were used to process the EEG data. We applied a high-pass filter at 0.1 Hz, followed by a notch filter at 60 Hz and harmonics of 60 Hz to each participant's raw EEG data. We then performed three preprocessing steps (Nolan, Whelan, & Reilly, 2010) to identify electrodes with severe artifacts. First, we calculated the mean correlation between each electrode and all other electrodes as electrodes should be moderately correlated with other electrodes because of volume conduction. We z-scored these means across electrodes and rejected electrodes with z scores less than -3. Second, we calculated the variance for each electrode as electrodes with very high or low variance across a session are likely dominated by noise or have poor contact with the scalp. We then z-scored variance across electrodes and rejected electrodes with a $|z| \geq 3$. Finally, we expect many electrical signals to be autocorrelated, but signals generated by the brain versus noise are likely to have different forms of autocorrelation. Therefore, we calculated the Hurst exponent, a measure of long-range autocorrelation, for each electrode and rejected electrodes with a $|z| \geq 3$. Electrodes marked as bad by this procedure were excluded from the average rereference. We then calculated the average voltage across all remaining electrodes at each time sample and rereferenced the data by subtracting the average voltage from the filtered EEG data. We used wavelet-enhanced independent component analysis (Castellanos & Makarov, 2006) to remove artifacts from eyeblinks and saccades.

EEG Data Microstate Analysis

We applied a bandpass filter of 1–40 Hz and then downsampled the artifact-corrected mnemonic state task and resting-state data to 250 Hz. Data were normalized by subtracting and dividing by the mean and standard deviation voltage, respectively, across time. Our microstate analysis, performed via custom Python code based on a publicly available microstate toolbox (Poulsen, Pedroni, Langer, & Hansen, 2018), consists of four main steps (Figure 2). First, we identified subject-level microstates from each participant's resting-state data. Second, we identified group-level microstates by aggregating the individual participant microstates. Third, we applied the group-level microstates to each participant's mnemonic state data to identify sample-specific microstates during memory encoding and memory retrieval. Finally, we extracted microstate properties from the mnemonic state data.

Participant-level Microstate Identification

From each participant's resting-state data, we identified n-clusters of microstates using a modified k-means clustering algorithm (Murray et al., 2008). First, we calculated the global field power (GFP) and extracted all GFP peaks. GFP is the standard deviation of the voltage across all electrodes at each time point (Skrandies, 1990) and is a reference-independent measure of the strength of the electrophysiological response (Murray et al., 2008). GFP peaks reflect periods of momentary stability in the topography (Zanesco, 2020). We used the SciPy signal module to identify the GFP peaks. Next, the GFP peaks were submitted to a modified k-means clustering algorithm (Poulsen et al., 2018) to identify the best fitting n clusters or microstate template maps (Pascual-Marqui, Michel, & Lehmann, 1995). We repeated these steps for sets of clusters, with the number of clusters ranging from 2 to 12 (Zanesco, Denkova, & Jha, 2021a).

To identify the number of clusters n that best fit a participant's data, we used five criteria: Silhouettes, Davies and Bouldin, Point-Biserial, Dunn, and Cross-Validation criterion based on previous work, which has established the use of a metacriterion for assessing the optimal number of clusters (Bréchet, Brunet, Perogamvros, Tononi, & Michel, 2020; Bréchet et al., 2019; Custo et al., 2017). Each of the five criteria provides a fit value for each cluster set, and a cluster set is considered the best if it has either the highest value (Silhouettes, Point-Biserial, and Dunn) or the lowest value (Davies and Bouldin, and Cross-Validation; Charrad, Ghazzali, Boiteau, & Niknafs, 2014). Silhouettes assesses the distance between each cluster, such that larger values reflect more distant or separable clusters indicating better fit (Rousseeuw, 1987). We used the sklearn metrics module to calculate Silhouettes. The Point-Biserial correlation assesses the relative distance for within-cluster versus between-clusters samples (Milligan, 1981, 1980); the between-clusters sample distance should be greater than the within-cluster sample distance. Therefore, to the extent that the identified clusters provide an optimal fit for the data, the dissimilarity value for between-clusters samples should be higher than within-cluster samples and thus a larger Point-Biserial value (between − within) indicates a better fit. We utilized the *pointbiserialr* module

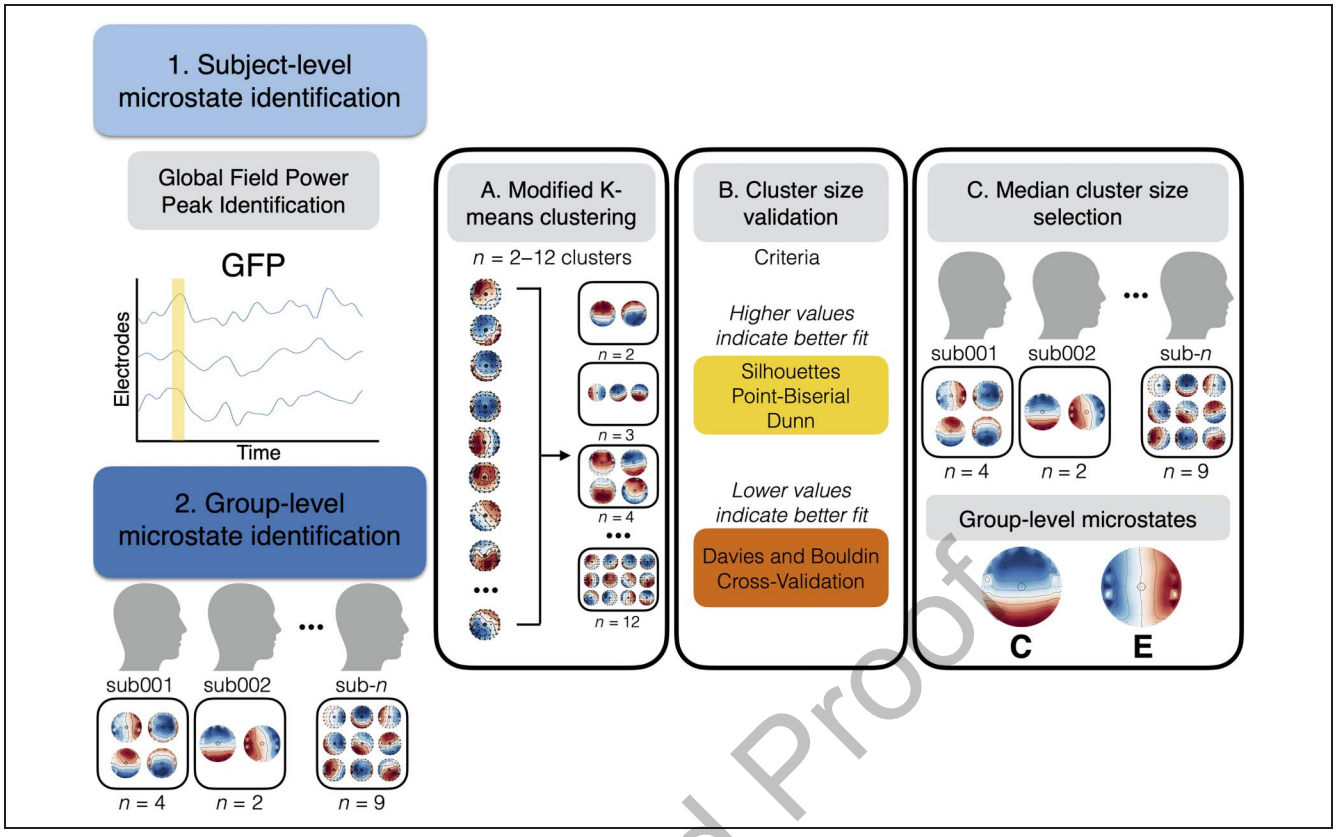

Figure 2. Microstates: procedure and results. (1) We first identified subject-level microstates. From each participant's resting-state data, we extracted the global field power (GFP) peaks. (A) We submitted these peaks to a modified k-means clustering algorithm with the number of possible clusters ranging from 2 to 12. (B) We used five criteria, Silhouettes, Davies and Bouldin, Point-Biserial, Dunn, and Cross-Validation, to evaluate the fit of these 2 to 12 clusters. Each criterion provided a best fitting number of clusters. For the criteria in yellow (Silhouettes, Point-Biserial, Dunn), higher values indicate better fit; for the criteria in orange (Davies and Bouldin, Cross-Validation), lower values indicate better fit. (C) Cluster size selection was performed by selecting the median best fitting n clusters across the five criteria. As an example, if the five criteria resulted in the best fitting n clusters: n = 2, 5, 6, 8, 10, the median cluster size selection would be n = 6. The outcome of this step resulted in a single n cluster set that best fit the participant's mnemonic state data. (2) After identifying the best n fitting microstates for each participant, we subjected the subject-level microstate maps to the same procedure of (A) modified k-means clustering followed by (B) cluster size validation and (C) median cluster size selection. As a result of this process, we identified two group-level microstates in the resting-state data. We use the naming convention employed in previous research to facilitate interpretation and comparison across data sets.

within the SciPy package to calculate the Point-Biserial correlation. Dunn evaluates the ratio of pairwise distances for within-cluster and between-clusters samples (Dunn, 1974). As with Point-Biserial, a large value for Dunn indicates greater cluster separation, with higher within-cluster relative to between-clusters similarity indicating a better fit. We utilized the *validcluster* package to calculate Dunn. Davies and Bouldin assesses within- versus between-clusters separation (Davies & Bouldin, 1979), and a smaller value is preferred as it indicates more separation between relative to within clusters. We used the *sklearn* metrics module to calculate the Davies and Bouldin score. Cross-Validation assesses the residual noise between the derived template maps and the actual data (Tzovara et al., 2012; Pascual-Marqui et al., 1995), and a lower value indicates better fit. We utilized the code provided in Poulsen and colleagues (2018) to calculate the Cross-Validation (Poulsen et al., 2018). To identify the best fitting cluster set across the five criteria, we calculated the median of the identified cluster set sizes. Theoretically, for each individual criteria, different cluster sets provide the best fit, for example, n = 2, 5, 6, 8, 10; in this example, the best fit would be n = 6 clusters. We repeated this process for each participant to identify subject-level microstates.

Group-level Microstate Identification

We next identified group-level microstates. We submitted all subject-level microstate maps to the modified *k*-means clustering algorithm above and identified the best fitting microstates across participants using the same process as subject-level microstate identification with the same five criteria.

Sample-level Microstate Assignment

Next, we assigned each sample within the mnemonic state task a microstate label. First, for each individual participant, we segmented the mnemonic state task trials. The segmentation window began at stimulus onset and

spanned the duration of the stimulus (2000 msec), yielding 500 time samples per trial. We then individually correlated each of the 500 time samples in a given trial with each of the group-level microstate maps. We calculated the absolute value of the resulting Pearson's r, and a sample was labeled with the most correlated microstate except in cases in which none of the resulting r values exceeded a threshold of 0.5 (Custo et al., 2017). We retained the original sign of the correlation to account for polarity in all subsequent analyses (Tamano, Ogawa, Katagiri, Cai, & Asai, 2022). We performed an additional round of thresholding based on the temporal extent of a given microstate (accounting for polarity). By definition, a microstate is sustained, meaning that the same microstate should be present for multiple consecutive samples. We required a given microstate to be present for six consecutive samples (a minimum of 24 msec; Zanesco et al., 2021a). In all other cases (i.e., no r values exceeding .5 and insufficient contiguous microstates), the sample was unlabeled and excluded from the analysis.

Mnemonic State Task Microstate Properties

We analyzed two microstate properties when assessing the extent to which microstates vary across memory brain states: duration and coverage. Duration represents how long, on average, a microstate persists in milliseconds following its onset. Because we require a microstate to be present for at least six consecutive samples, the minimum duration is 24 msec. With resting-state data, coverage reflects the fraction of total recording time for which a given microstate is dominant (Michel & Koenig, 2018); however, because we are using event-related data, the fraction is based on the time interval under investigation. To assess general microstate dissociations across conditions, we measured coverage across the 2000-msec stimulus interval. In the context of our mnemonic state task, if a microstate was active for 1000 msec throughout the 2000-msec stimulus interval, the coverage of the microstate would be 50%. We aggregated the duration and coverage values across all participants separately for encode and retrieve trials. As a result, multiple microstates may have nonzero coverage in the same time interval. Coverage should therefore be interpreted as the percentage of time in the specified interval during which the microstate is active, on average, across trials and across participants. We additionally assessed coverage for 100-msec time windows across the stimulus interval and used a sliding window approach to improve visualization. We slid the 100-msec time windows every 10 msec, resulting in 191 total time windows. We performed statistics exclusively on the twenty 0-centered nonoverlapping time windows (e.g., 0–100 msec, 100–200 msec).

Statistical Analyses

To assess microstate dissociations across encode and retrieve trials, as well as over time, we conducted repeated-measures ANOVAs. We conducted post hoc ANOVAs and t tests for significant main effects and interactions. For post hoc comparisons across microstates and across time, we used false discovery rate (FDR; $p = .05$) correction (Benjamini & Hochberg, 1995) to correct for multiple comparisons.

RESULTS

Two Microstates Fit the Resting-state Data

Our first goal was to identify microstates in the resting-state data. We identified the best fitting n microstates that characterized the group-level resting-state data, resulting in the identification of two microstates (Figure 2). To facilitate interpretation and comparison with prior work, we have adopted the naming conventions used in previous research and label these Microstates C and E (Custo et al., 2017), although we note that multiple topographies have been assigned the label "E" in the literature; we expand upon this point in the Discussion. The two microstates that we identified have previously been associated with particular RSNs identified via source-localization and fMRI data: the saliency network (Microstate C) and the DMN (Microstate E; Custo et al., 2017; Britz et al., 2010).

Microstates C and E Track Encoding and Retrieval

Our primary goal was to assess the extent to which the two microstates identified in the resting-state data dissociate memory encoding and memory retrieval. A longer microstate duration for a specific memory state would suggest that sustained network engagement supports either encoding or retrieval. We measured the duration of each microstate during the 2000-msec List 2 stimulus interval. We found significant dissociations in microstate duration across encode and retrieve trials (Figure 3A). We conducted a 2 × 2 × 2 repeated-measures ANOVA with Instruction (encode, retrieve), Microstate (C, E), and Polarity (positive, negative) as factors. We found a main effect of Instruction, $F(1, 98) = 15.85$, $p < .001$, $\eta_p^2 = .14$. This effect was driven by overall greater duration across microstates for retrieve compared with encode trials. We did not find a main effect of Microstate, $F(1, 98) = 0.05$, $p = 0.83$, $\eta_p^2 < .001$, or Polarity, $F(1, 98) = 0.15$, $p = .70$, $\eta_p^2 = .002$. We found an interaction between Instruction and Microstate, $F(1, 98) = 25.13$, $p < .001$, $\eta_p^2 = .20$. We did not find interactions between Instruction and Polarity, $F(1, 98) = 1.93$, $p = .17$, $\eta_p^2 = .02$; Microstate and Polarity, $F(1, 98) = 0.63$, $p = .43$, $\eta_p^2 = .006$; or a three-way interaction between Instruction, Microstate, and Polarity, $F(1, 98) = 1.00$, $p = .32$, $\eta_p^2 = .01$. Bayes Factor analysis indicated that a model without the three-way interaction term is preferred to a model with the three-way interaction term by a factor of >100. We performed follow-up post hoc paired t tests to investigate encode versus

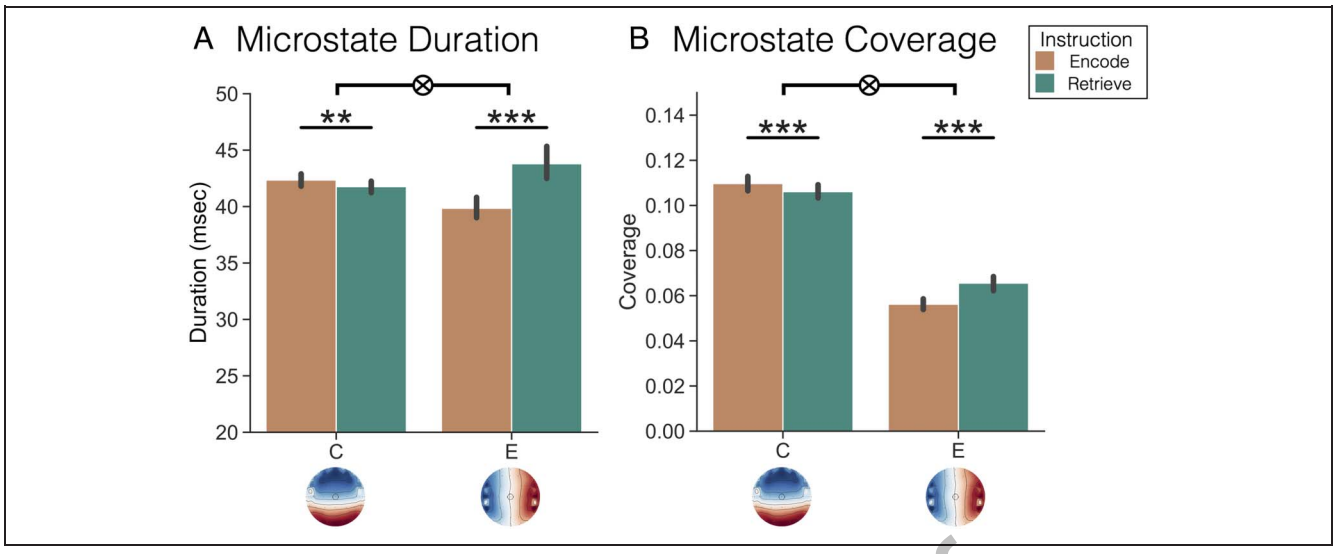

Figure 3. Microstate duration and coverage as a function of instruction. (A) Microstate E has a significantly longer duration during retrieve (teal) compared with encode (orange) trials; Microstate C has a significantly longer duration during encode compared with retrieve trials. (B) Microstate E coverage is greater for retrieve compared with encode trials; Microstate C coverage is greater for encode compared with retrieve trials. Error bars reflect standard error of the mean. $^{**}p < .01$; $^{***}p < .001$ (FDR-corrected).

retrieve dissociations for each microstate and averaged duration across polarity. Microstate duration was significantly greater for encode compared with retrieve trials for Microstate C, $t(98) = 2.76$, $p = .007$, Cohen's $d = 0.11$ (FDR-corrected) and for retrieve compared with encode trials for Microstate E, $t(98) = 4.65$, $p < .001$, Cohen's $d = 0.33$ (FDR-corrected).

We next sought to directly compare condition-driven duration dissociations across microstates. We computed duration difference scores (retrieve − encode) for each microstate. We found that the duration difference in Microstate E ($M = 3.95$, $SD = 8.46$) is significantly greater than the duration difference in Microstate C ($M = -0.59$, $SD = 2.11$; $t(98) = 5.01$, $p < .001$, Cohen's $d = 0.74$; FDR-corrected). These results indicate that Microstate E duration is specifically increased for retrieve trials whereas Microstate C duration is specifically increased for encode trials.

Having shown that microstate duration varies as a function of instruction, we next sought to assess whether microstate coverage likewise differs across encode and retrieve trials. Greater coverage selectively for encoding or retrieval would suggest that a microstate is more engaged or active during that specific memory state and could be observed even in the absence of a between-conditions difference in duration. We measured the coverage of each microstate during the 2000-msec List 2 stimulus interval and found significant dissociations in coverage across encode and retrieve trials (Figure 3B). We conducted a 2 × 2 × 2 repeated-measures ANOVA with Instruction (encode, retrieve), Microstate (C, E), and Polarity (positive, negative) as factors and coverage as the dependent variable. We found a main effect of Instruction, $F(1, 98) = 9.51$, $p = .003$, $\eta_p^2 = .09$, driven by greater coverage across microstates for encode compared with retrieve trials. We found a main effect of Microstate, $F(1, 98) = 166.26$, $p < .001$, $\eta_p^2 = .63$, driven by greater coverage for Microstate C compared with Microstate E. We did not find a main effect of Polarity, $F(1, 98) = 0.90$, $p = .35$, $\eta_p^2 = .01$. We found an interaction between Instruction and Microstate, $F(1, 98) = 21.39$, $p < .001$, $\eta_p^2 = .18$. We did not find an interaction between Instruction and Polarity, $F(1, 98) = 3.03$, $p = .08$, $\eta_p^2 = .03$; Microstate and Polarity, $F(1, 98) = 3.16$, $p = .08$, $\eta_p^2 = .03$; or a three-way interaction between Instruction, Microstate, and Polarity, $F(1, 98) = 0.46$, $p = .50$, $\eta_p^2 = .005$. Bayes Factor analysis indicated that a model without the three-way interaction term is preferred to a model with the three-way interaction term by a factor of > 100. We performed follow-up post hoc paired t tests to investigate encode versus retrieve dissociations for each microstate and averaged coverage across polarity. Microstate coverage was significantly greater for encode compared with retrieve trials for Microstate C, $t(98) = 4.14$, $p < .001$, Cohen's $d = 0.11$ (FDR-corrected) and for retrieve compared with encode trials for Microstate E, $t(98) = 4.22$, $p < .001$, Cohen's $d = 0.33$ (FDR-corrected).

We next sought to directly compare condition-driven coverage dissociations across microstates. We computed coverage difference scores (retrieve − encode) for each microstate. We found that the coverage difference in Microstate E ($M = .009$, $SD = .02$) is significantly greater than the coverage difference in Microstate C ($M = -.004$, $SD = .009$; $t(98) = 4.63$, $p < .001$, Cohen's $d = 0.77$; FDR-corrected). These results indicate that Microstate E coverage is specifically increased for retrieve trials whereas Microstate C coverage is specifically increased for encode trials.

Together, the duration and coverage results reveal that memory states are characterized by opposing patterns of

microstate engagement whereby Microstate E tracks retrieval and Microstate C tracks encoding.

Memory State Temporal Dynamics

Our analyses above provide strong evidence that encode and retrieve trials are distinguished by the engagement of Microstates C and E. Microstate C is more engaged, both in terms of duration and coverage, during encode compared with retrieve trials whereas Microstate E shows the opposite pattern. Critically, however, these results do not indicate when during the trial Microstates C and E engagement dissociates the two instructions. Microstate engagement may either be sustained throughout the stimulus interval or engagement may fluctuate over time. To test these two alternatives, we recalculated coverage for Microstates C and E in 100-msec time intervals spanning the stimulus interval (2000 msec). Our approach was similar to that used in our prior coverage analysis (see Methods section); however, we used a sliding window and calculated the coverage separately for each 100-msec time window every 10 msec. We only performed statistics on the 20 non-overlapping windows (0–100 msec, 100–200 msec, etc.). Although two microstates cannot be assigned to the same time sample, it is possible to find nonzero coverage for multiple microstates in a single time window because of averaging across both trials and participants. Given the lack of an effect of polarity in the prior analysis, polarity is ignored for all coverage analyses below.

We found greater Microstate C coverage for encode compared with retrieve trials around 500–1000 msec following stimulus onset (Figure 4, top). We conducted a 2 × 20 repeated-measures ANOVA with Instruction (encode, retrieve) and Time Interval (non-overlapping) as factors and coverage as the dependent variable. We found a main effect of Instruction, $F(1, 98) = 23.18, p < .001, \eta_p^2 = .19$, consistent with our coverage analysis above, and a main effect of Time Interval, $F(19, 1862) = 6.41, p < .001, \eta_p^2 = .06$. We found an interaction between Instruction and Time Interval, $F(19, 1862) = 1.69, p = .03, \eta_p^2 = .02$. We performed post hoc paired t tests at each time interval and used FDR correction ($p = .05$) to correct for multiple comparisons. The coverage dissociation between encode and retrieve trials was significant in three intervals (500–

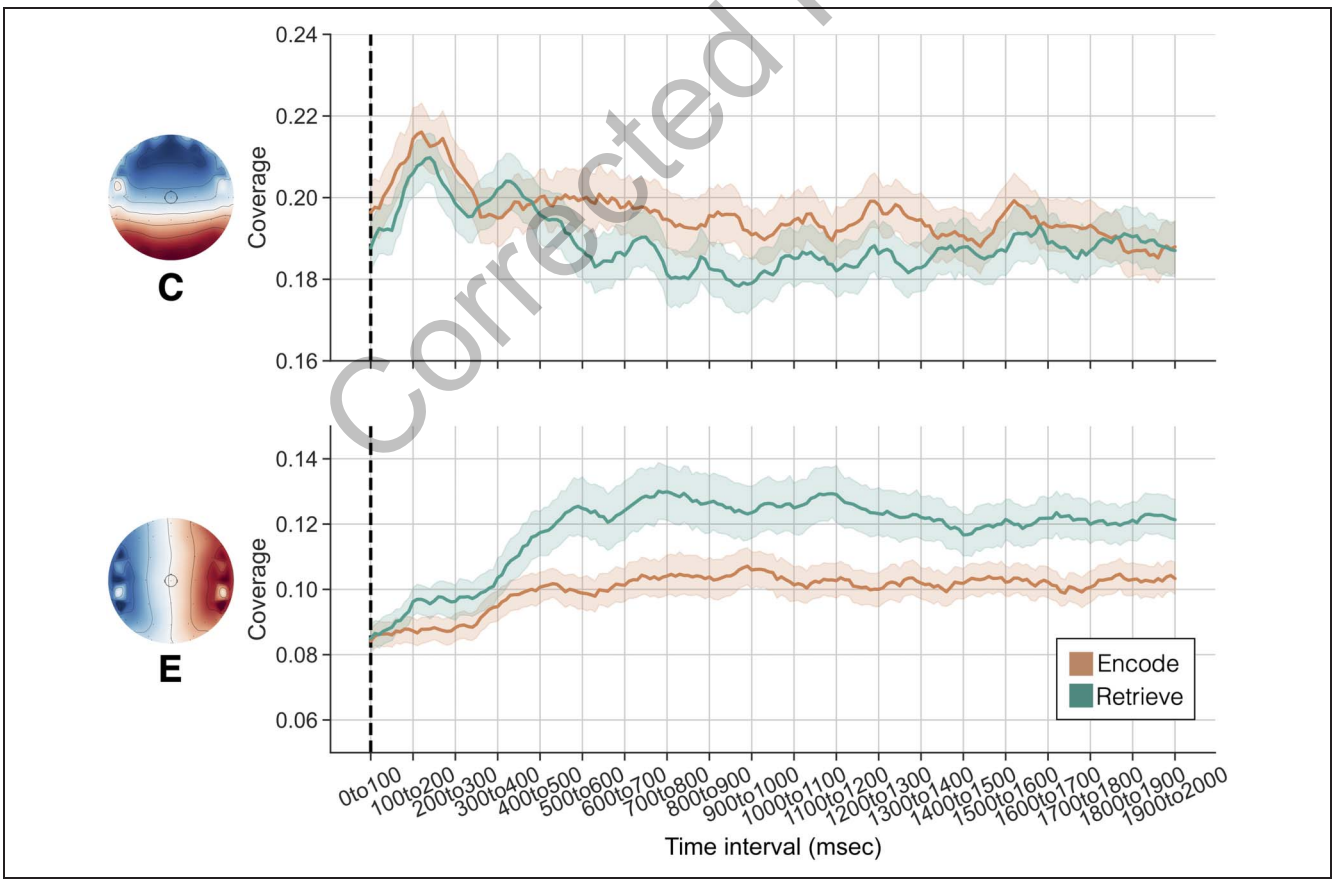

Figure 4. Temporal dynamics of Microstate C and E coverage. We examined Microstate C and E coverage throughout the stimulus interval separately for encode (orange) and retrieve (teal) trials. Stimulus onset at 0–100 msec is indicated by the vertical dashed line. Microstate C coverage is greater during encode compared with retrieve trials during three time intervals (500–600 msec; 800–900 msec; 1200–1300 msec). Microstate E coverage is greater during retrieve compared with encode trials for all intervals excluding 0–100 msec and 200–400 msec. The shaded area represents the standard error of the mean.

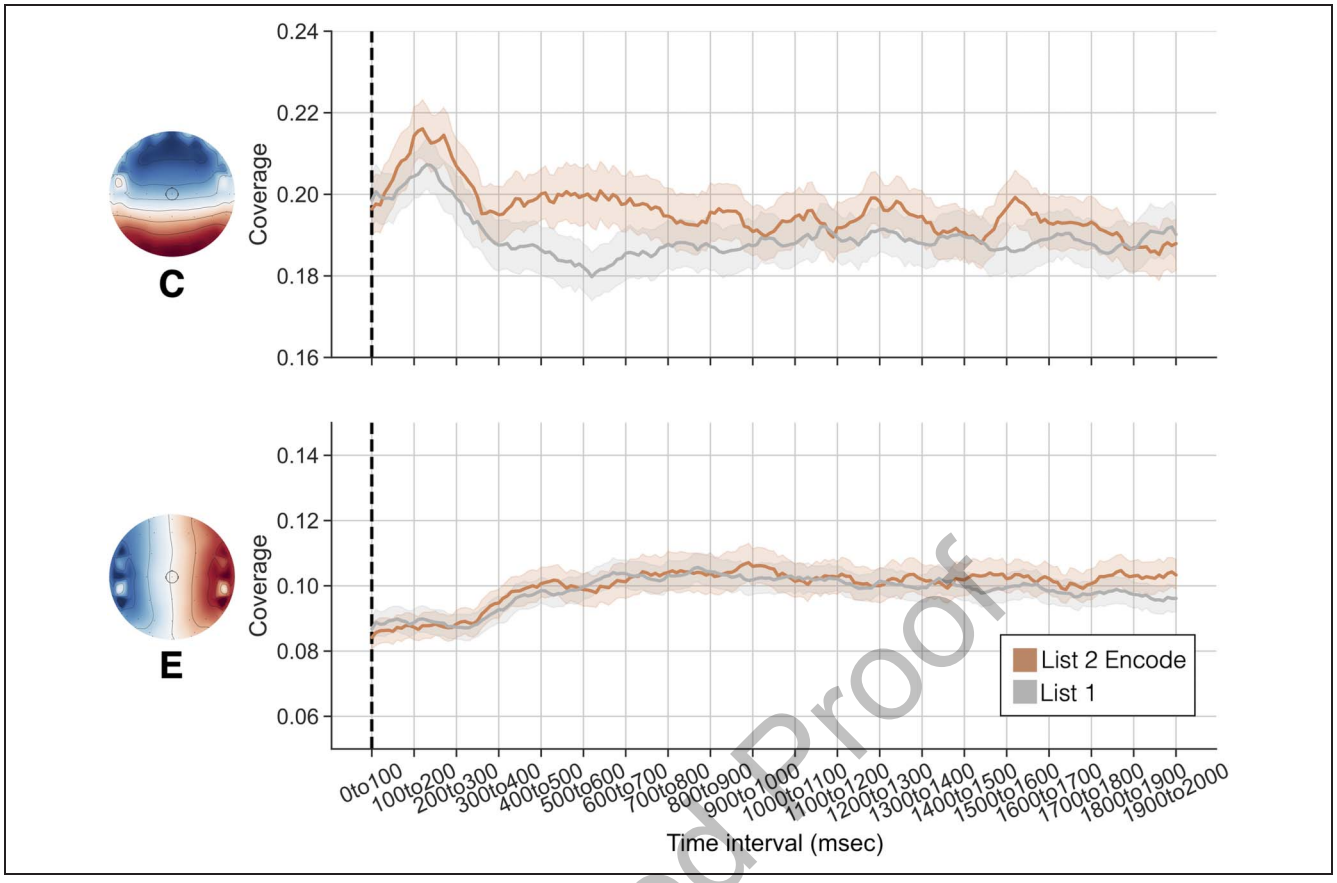

Figure 5. Temporal dynamics of List 1 versus List 2 encode trials. We compared microstate coverage across List 2 encode (orange) and List 1 (gray) trials. Note that the *y* axes differ across panels, as average microstate coverage (irrespective of condition) is variable. Stimulus onset at 0–100 msec is indicated by the vertical dashed line in each panel. Microstate C coverage is greater on List 2 encode compared with List 1 trials during the 400- to 700-msec interval. Microstate E coverage did not significantly differ between the two conditions. The shaded area represents the standard error of the mean.

600: $t(98) = 2.68$, $p = .009$, Cohen's $d = 0.18$; 800–900: $t(98) = 2.62$, $p = .01$, Cohen's $d = 0.19$; 1200–1300: $t(98) = 2.60$, $p = .01$, Cohen's $d = 0.19$; FDR-corrected). No other intervals survived FDR correction ($|ts| < 2.87$, $ps > .005$).

We found greater Microstate E coverage for retrieve compared with encode trials throughout the stimulus interval (Figure 4, bottom). We conducted a 2 × 20 repeated-measures ANOVA with Instruction (encode, retrieve) and Time Interval as factors and coverage as the dependent variable. We found a main effect of Instruction, $F(1, 98) = 18.36$, $p < .001$, $\eta_p^2 = .16$, consistent with our coverage analysis above, and a main effect of Time Interval, $F(19, 1862) = 15.09$, $p < .001$, $\eta_p^2 = .13$. We found an interaction between Instruction and Time Interval, $F(19, 1862) = 3.10$, $p < .001$, $\eta_p^2 = .03$. We performed post hoc paired *t* tests at each time interval and used FDR correction ($p = .05$) to correct for multiple comparisons. The coverage dissociation between encode and retrieve trials was significant at all time intervals excluding the 0- to 100-msec and 200- to 400-msec intervals ($|ts| < 1.94$, $ps > .05$).

Together, these results suggest that memory states are supported by a transient increase in Microstate C and sustained engagement (or disengagement, in the case of encode trials) of Microstate E.

Microstate Dissociations between List 1 and List 2 Encode Trials

Our interpretation is that, compared with retrieval, encoding is characterized by increased engagement of Microstate C and decreased engagement of Microstate E. However, it is conceivable that microstate coverage and duration on encode trials reflects interference detection and/or a top–down driven inhibition of retrieval, rather than encoding per se. On all List 2 trials, regardless of instruction, there is the potential for retrieval given the presence of recently presented categorically associated stimuli. Indeed, we have found evidence for automatic retrieval of List 1 objects during List 2 trials regardless of instruction (Smith et al., 2022). Therefore, to claim that microstate dissociations specifically reflect memory encoding, it is necessary to measure microstate engagement when there is little (or no) potential for retrieval. The List 1 trials present just such an opportunity. Although there are no trial-level cues, the List 1 trials are analogous

to the List 2 encode trials in terms of memory demands, as participants were instructed to form a memory of each List 1 object; however, there should be no interference and no need for retrieval inhibition on these trials.

To assess the extent to which List 2 encode trials reflect general "encoding" as opposed to interference-driven retrieval-suppression, we measured coverage in each of the two microstates in 100-msec time intervals spanning the stimulus interval, separately for List 1 and List 2 encode trials (Figure 5). We again used a sliding window for visualization and report statistics for the 20 non-overlapping windows. To test for microstate dissociations, we conducted two—one per microstate—2 × 20 repeated-measures ANOVAs with Condition (List 1, List 2 encode) and Time Interval as factors and coverage as the dependent variable.

Both microstates showed main effects of Time Interval (Fs > 6.18, ps < .001). Microstate C showed a main effect of Instruction, $F(1, 98) = 11.79, p = .001, \eta_p^2 = .11$, driven by greater coverage for List 2 encode trials compared with List 1 trials. Microstate C also showed significant interactions between Instruction and Time Interval, $F(19, 1862) = 2.03, p = .006, \eta_p^2 = .02$. We performed post hoc paired t tests at each time interval and used FDR correction ($p = .05$) to correct for multiple comparisons for Microstate C. Microstate C coverage was greater for List 2 encode compared with List 1 trials during the 400- to 700-msec interval (ts > 2.86, ps < .005). For Microstate E, we found no main effect of Instruction, $F(1, 98) = 0.60, p = 0.44, \eta_p^2 = .006$, and no interaction between Instruction and Time Interval, $F(19, 1862) = 0.93, p = .55, \eta_p^2 = .01$.

List 1 and List 2 encode trials most strongly dissociate in terms of Microstate C, which is more engaged, particularly early (500 msec) in the stimulus interval, during List 2 encode trials compared with List 1 trials. Given that Microstate E engagement was generally similar across List 1 and List 2 encode trials, this suggests that the Microstate E effects on List 2 encode trials are not merely a suppression of retrieval and instead broadly reflect encoding.

DISCUSSION

The goal of the present study was to investigate the spatiotemporal dynamics of memory states. Memory encoding and memory retrieval states can be dissociated by cortical network activity patterns (Smith et al., 2022; Long & Kuhl, 2021, 2019); however, whether memory states are supported by sustained activity in a specific network or by fluctuations across networks has remained an open question. By assessing the engagement of microstates, sustained global patterns of voltage scalp topographies (Michel & Koenig, 2018), we find that Microstate E, a potential analog of the DMN, dissociates memory states and shows temporally sustained engagement during retrieval compared with encoding. Microstate C, potentially reflecting the VAN, shows transient dissociations between memory states that may reflect control and/or attentional processes. Together, these results suggest that memory states, like other brain states, are supported by the maintenance of specific network configurations. These findings have implications for memory behavior and cognition more broadly, suggesting that hyper- or hypo-engagement of Microstate E may lead to over- or under-engagement of the memory retrieval state.

We find that Microstate E dissociates memory encoding and memory retrieval states. Microstate E duration and coverage are significantly greater during retrieval compared with encoding. Thus, Microstate E is more engaged and, once active, stays engaged for longer during retrieve trials. Two alternative versions of Microstate "E" have been identified in the literature. In some studies, Microstate E is characterized by a circumscribed posterior versus broader left/right/anterior gradient (Tomescu et al., 2022; Zanesco, Denkova, & Jha, 2021b; Zanesco, 2020; Damborská et al., 2019; Michel & Koenig, 2018) and is linked with the cingulo-opercular network or VAN. In these studies, Microstate E tracks on-task alertness (e.g., Zanesco et al., 2021b). In other studies, Microstate E is characterized by a left/right voltage gradient (Niu et al., 2022; Deolindo et al., 2021; Bréchet et al., 2019; D'Croz-Baron, Baker, & Michel, 2019; Custo et al., 2017)—as in the current study—and is linked with the DMN. Given that the Microstate E reported here is most consistent with the latter topography, our interpretation is that the Microstate E we have identified reflects the DMN. Activity increases in the DMN during episodic memory retrieval (Kim, 2010), semantic processing (Binder et al., 2009), and internally directed attention (Buckner & DiNicola, 2019). In addition, activity patterns in the DMN also support retrieval-mediated prediction (Long, Lee, & Kuhl, 2016), accessing of schematic information (Preston & Eichenbaum, 2013; van Kesteren, Ruiter, Fernández, & Henson, 2012), and reliance on prior conceptual knowledge (González-García & He, 2021). Thus, our findings are highly consistent with the existing literature, as the retrieve condition in the current study may tap into any or all of these processes; participants are instructed to retrieve a semantically associated stimulus encountered previously in the experiment. Which specific cognitive process Microstate E engagement is supporting—or whether all of these processes constitute "internal mentation"—is an important question for future work, as is the distinction between the different topographies of Microstate E.

Microstate E engagement during retrieval is sustained throughout the stimulus interval. Aside from the first 400 msec following stimulus onset—when participants are likely perceiving the stimulus in order to know which prior stimulus to retrieve—Microstate E coverage is greater during retrieve compared with encode trials. Connectivity between the DMN and other cortical networks (e.g., the DAN and FPCN) is thought to support internal attention (Kam et al., 2019), working memory (Murphy et al., 2020), and search during free recall (Kragel & Polyn, 2013). The methodological approach for

assessing microstates is winner-take-all such that only one microstate can be active at any given time sample. Thus, by definition, it is not possible to demonstrate concurrent engagement of multiple microstates at the level of time samples. However, we might have anticipated changes in network engagement over time such that microstate coverage would fluctuate throughout the stimulus interval. Although there may be conditions in which such fluctuations could be observed, in the current study with explicit instructions to retrieve a prior stimulus, we find that retrieval is characterized by sustained engagement of Microstate E. This finding has implications for future investigations into how memory states impact behavior. Hyper- or hypo-engagement of Microstate E may result in too much or too little retrieval, respectively, which may negatively impact memory success.

The sustained microstate engagement that we observe occurs on a slower timescale than hippocampally mediated encoding/retrieval dissociations. Rodent electrophysiology and theoretical models show that encoding and retrieval rely on distinct and opposing circuitry within the hippocampus and are governed by theta oscillations (Hasselmo, 2005; Hasselmo, Bodelon, & Wyble, 2002). Memory reactivation has been linked to specific phases of the theta oscillation (Kerrén, Linde-Domingo, Hanslmayr, & Wimber, 2018), and competing memories are reactivated during different phases of the theta cycle compared with to-be-encoded targets (Kerrén, van Bree, Griffiths, & Wimber, 2022), indicating that encoding and retrieval can fluctuate on the order of milliseconds. Although we expect that there is a link between hippocampal and cortical states—potentially signals emanating from the hippocampus are projected to the cortex—our interpretation of the present findings is that they do not directly reflect hippocampal theta signals and instead occur along a different, and longer, timescale. Indeed, prior work has not found a clear link between specific frequencies and microstates (Britz et al., 2010) and instead suggests that microstates are broadband in nature (Michel & Koenig, 2018). Hippocampal state changes are linked to changes in acetylcholine (ACh) that occur on the order of seconds, rather than milliseconds (Meeter, Murre, & Talamini, 2004), and there is evidence that ACh biases the memory system (Douchamps, Jeewajee, Blundell, Burgess, & Lever, 2013; Hasselmo, 2006). Although we do not measure ACh in the current study, we expect that the microstates we observe occur along a similar timescale and reflect slower memory state changes. This slower timescale means that sustained engagement of Microstate E has the potential to impact not only processing of the current stimulus, but subsequently encountered stimuli insofar as memory states linger in time (Patil & Duncan, 2018; Duncan, Sadanand, & Davachi, 2012)—presenting an important question for future investigation into the impact of memory states on downstream processing.

Decreased Microstate E engagement is a general property of an encoding state. Our mnemonic state task is designed such that on every trial with an explicit instruction, participants could engage in either an encoding or retrieval state; the instructions are intended to bias participants to one of these states. Although the mnemonic state task is ideally suited to distinguishing encoding and retrieval states given the matched perceptual and behavioral demands, a consequence of this design is that signals during encode trials could reflect interference detection or retrieval suppression rather than encoding per se. To demonstrate that decreased Microstate E coverage is a general property of encoding, and not because of interference-mediated retrieval suppression, we measured Microstate E coverage during trials in which retrieval was unlikely (if not impossible) and participants' goal was to encode the stimuli. We find that Microstate E coverage does not significantly differ across both types of encoding trials, a result that is consistent with the interpretation that decreased Microstate E engagement reflects a general encoding state, rather than top–down suppression of a retrieval state. However, the current study cannot address whether these effects extend beyond explicit or goal-directed memory states, as throughout the experiment, participants had explicit goals to encode or retrieve. Microstate E and the DMN have been linked to spontaneous thought and mind wandering (Higgins et al., 2021; Bréchet et al., 2019; Andrews-Hanna, Reidler, Sepulcre, Poulin, & Buckner, 2010), suggesting that such signals may be a more general marker of the internal axis of attention (Chun, Golomb, & Turk-Browne, 2011). The engagement of microstates in incidental or automatic encoding and retrieval, as well as more broadly in the service of external versus internal attention, is an important avenue for future research.

Microstate C engagement transiently increases during encoding compared with retrieval states. Microstate C has previously been linked to the saliency network or VAN (Britz et al., 2010). The VAN is engaged during cognitive control or executive function tasks (Dosenbach et al., 2006) and is thought to reflect bottom–up attention (Corbetta & Shulman, 2002). Thus, Microstate C engagement in the present study may reflect an interference detection response to the competing stored representation on encode trials (e.g., Kuhl, Bainbridge, & Chun, 2012). This detection may be carried out by the ACC, a region that is part of Microstate C. This interpretation is supported by our finding of greater Microstate C coverage during encoding trials in which retrieval was possible versus trials in which retrieval was not possible. Specifically, we find greater Microstate C coverage 400–700 msec following stimulus onset, potentially reflecting interference detection following identification of the stimulus. Given the current study design, we are unable to measure stimulus-specific representations; thus, Microstate C engagement may reflect a suppression of a retrieved prior stimulus and/or a suppression of the retrieval state itself, as we have previously found that automatic retrieval can occur in the absence of successful retrieval (Smith et al.,

2022). In summary, whereas Microstate E generally tracks memory state engagement, putative attentional processes are differentially engaged when there is potential retrieval competition.

The exact nature of and relationship between resting-state versus task-derived microstates remains an important open question. Here, we have used microstates derived from resting-state data and have back-fit these microstates to our mnemonic task data. There is evidence that networks identified during rest are not identical to those identified during tasks (Davis, Stanley, Moscovitch, & Cabeza, 2017), suggesting that there may exist distinct resting versus cognitive networks. However, given the expectation that microstates form the "basis of cognition" (Seitzman et al., 2017), and that we have previously observed memory state dissociations in large-scale cortical networks using task-based fMRI data (Long & Kuhl, 2021), we expected that resting-state-derived microstates should be engaged in the mnemonic state task. In line with this expectation, we find that microstates, which have previously been identified from spontaneous continuous EEG signals (e.g., Bréchet et al., 2019; Custo et al., 2017), are differentially engaged depending on the state of the memory system. Our current approach does leave open the question of whether there are task-specific microstates that dissociate memory states, although prior work did not find significant differences between resting-state-derived microstates versus those derived during a working memory task (Tamano et al., 2022). Future work is necessary to disentangle task-specific from resting-state-derived patterns of network activity.

In summary, memory encoding and memory retrieval are differentiated by the sustained engagement of a putative DMN microstate. The tendency to over- or under-engage this microstate may account for intra- and inter-individual variability in memory success. More broadly, sustained engagement of Microstate E may impact other cognitive processes via its role in internally directed attention.

Acknowledgments

Nicole Long is an iTHRIV Scholar. The iTHRIV Scholars Program is supported in part by the National Center for Advancing Translational Sciences of the National Institutes of Health under Award Numbers UL1TR003015 and KL2TR003016.

Reprint requests should be sent to Nicole M. Long, Department of Psychology, University of Virginia 22904, or via e-mail: niclong@virginia.edu.

Data Availability Statement

The raw, de-identified data and the associated experimental and analysis codes used in this study can be accessed via the Long Term Memory laboratory website (https://longtermmemorylab.com).

Author Contributions

Yuju Hong: Conceptualization; Data curation; Formal analysis; Software; Visualization; Writing—Original draft; Writing—Review & editing. Isabelle L. Moore: Formal analysis; Software; Supervision; Visualization; Writing—Original draft; Writing—Review & editing. Devyn E. Smith: Formal analysis; Software; Supervision; Visualization; Writing—Original draft; Writing—Review & editing. Nicole M. Long: Conceptualization; Formal analysis; Funding acquisition; Project administration; Software; Supervision; Visualization; Writing—Original draft; Writing—Review & editing.

Funding Information

Nicole M. Long, National Center for Advancing Translational Sciences (https://dx.doi.org/10.13039/100006108), grant number: KL2TR003016, grant number: UL1TR003015.

Diversity in Citation Practices

Retrospective analysis of the citations in every article published in this journal from 2010 to 2021 reveals a persistent pattern of gender imbalance: Although the proportions of authorship teams (categorized by estimated gender identification of first author/last author) publishing in the *Journal of Cognitive Neuroscience* (*JoCN*) during this period were M(an)/M = .407, W(oman)/M = .32, M/W = .115, and W/W = .159, the comparable proportions for the articles that these authorship teams cited were M/M = .549, W/M = .257, M/W = .109, and W/W = .085 (Postle and Fulvio, *JoCN*, 34:1, pp. 1–3). Consequently, *JoCN* encourages all authors to consider gender balance explicitly when selecting which articles to cite and gives them the opportunity to report their article's gender citation balance. The authors of this article report its proportions of citations by gender category to be as follows: M/M = 0.522; W/M = 0.224; M/W = 0.149; W/W = 0.104.

REFERENCES

Andrews-Hanna, J. R., Reidler, J. S., Sepulcre, J., Poulin, R., & Buckner, R. L. (2010). Functional-anatomic fractionation of the brain's default network. *Neuron*, *65*, 550–562. https://doi.org/10.1016/j.neuron.201.02.005, PubMed: 20188659

Beaty, R. E., Chen, Q., Christensen, A. P., Qiu, J., Silvia, P. J., & Schacter, D. L. (2018). Brain networks of the imaginative mind: Dynamic functional connectivity of default and cognitive control networks relates to openness to experience. *Human Brain Mapping*, *39*, 811–821. https://doi.org/10.1002/hbm.23884, PubMed: 29136310

Benjamini, Y., & Hochberg, Y. (1995). Controlling the false discovery rate: A practical and powerful approach to multiple testing. *Journal of the Royal Statistical Society: Series B (Methodological)*, *57*, 289–300. https://doi.org/10.1111/j.2517-6161.1995.tb02031.x

Binder, J. R., Desai, R. H., Graves, W. W., & Conant, L. L. (2009). Where is the semantic system? A critical review and

meta-analysis of 120 functional neuroimaging studies. *Cerebral Cortex*, *19*, 2767–2796. https://doi.org/10.1093/cercor/bhp055, PubMed: 19329570

Bréchet, L., Brunet, D., Birot, G., Gruetter, R., Michel, C. M., & Jorge, J. (2019). Capturing the spatiotemporal dynamics of self-generated, task-initiated thoughts with EEG and fMRI. *Neuroimage*, *194*, 82–92. https://doi.org/10.1016/j.neuroimage.2019.03.029 PubMed: 30902640

Bréchet, L., Brunet, D., Perogamvros, L., Tononi, G., & Michel, C. M. (2020). EEG microstates of dreams. *Scientific Reports*, *10*, 17069. https://doi.org/10.1038/s41598-020-74075-z, PubMed: 33051536

Britz, J., Van De Ville, D., & Michel, C. M. (2010). BOLD correlates of EEG topography reveal rapid resting-state network dynamics. *Neuroimage*, *52*, 1162–1170. https://doi.org/10.1016/j.neuroimage.2010.02.052, PubMed: 20188188

Brunet, D., Murray, M. M., & Michel, C. M. (2011). Spatiotemporal analysis of multichannel EEG: Cartool. *Computational Intelligence and Neuroscience*, 813870. https://doi.org/10.1155/2011/813870, PubMed: 21253358

Buckner, R. L., & DiNicola, L. M. (2019). The brain's default network: Updated anatomy, physiology and evolving insights. *Nature Reviews Neuroscience*, *20*, 593–608. https://doi.org/10.1038/s41583-019-0212-7, PubMed: 31492945

Castellanos, N. P., & Makarov, V. A. (2006). Recovering EEG brain signals: Artifact suppression with wavelet enhanced independent component analysis. *Journal of Neuroscience Methods*, *158*, 300–312. https://doi.org/10.1016/j.jneumeth.2006.05.033, PubMed: 16828877

Charrad, M., Ghazzali, N., Boiteau, V., & Niknafs, A. (2014). Nbclust: An r package for determining the relevant number of clusters in a data set. *Journal of Statistical Software*, *61*, 1–36. https://doi.org/10.18637/jss.v061.i06

Chun, M. M., Golomb, J. D., & Turk-Browne, N. B. (2011). A taxonomy of external and internal attention. *Annual Review of Psychology*, *62*, 73–101. https://doi.org/10.1146/annurev.psych.093008.100427

Corbetta, M., & Shulman, G. L. (2002). Control of goal-directed and stimulus-driven attention in the brain. *Nature Reviews Neuroscience*, *3*, 201–215. https://doi.org/10.1038/nrn755, PubMed: 11994752

Custo, A., Van De Ville, D., Wells, W. M., Tomescu, M. I., Brunet, D., & Michel, C. M. (2017). Electroencephalographic resting-state networks: Source localization of microstates. *Brain Connectivity*, *7*, 671–682. https://doi.org/10.1089/brain.2016.0476, PubMed: 28938855

Damborská, A., Tomescu, M. I., Honzírková, E., Barteček, R., Honzírková, J., Fedeorová, S., et al. (2019). EEG resting-state large-scale brain network dynamics are related to depressive symptoms. *Frontiers in Psychiatry*, *10*, 548. https://doi.org/10.3389/fpsyt.2019.00548, PubMed: 31474881

Davies, D. L., & Bouldin, D. W. (1979). A cluster separation measure. *IEEE Transactions on Pattern Analysis and Machine Intelligence*, *1*, 224–227. https://doi.org/10.1109/TPAMI.1979.4766909

Davis, S. W., Stanley, M. L., Moscovitch, M., & Cabeza, R. (2017). Resting-state networks do not determine cognitive function networks: A commentary on Campbell and Schacter (2016). *Language, Cognition and Neuroscience*, *32*, 669–673. https://doi.org/10.1080/23273798.2016.1252847, PubMed: 28989941

D'Croz-Baron, D. F., Baker, M., & Michel, C. M. (2019). EEG microstates analysis in young adults with autism spectrum disorder during resting-state. *Frontiers in Human Neuroscience*, *13*, 173. https://doi.org/10.3389/fnhum.2019.00173, PubMed: 31244624

Deolindo, C. S., Ribeiro, M. W., de Aratanha, M. A. A., Scarpari, J. R. S., Foster, C. H. Q., da Silva, R. G. A., et al. (2021). Microstates in complex and dynamical environments: Unraveling situational awareness in critical helicopter landing maneuvers. *Human Brain Mapping*, *42*, 3168–3181. https://doi.org/10.1002/hbm.25426, PubMed: 33942444

Dosenbach, N. U., Visscher, K. M., Palmer, E. D., Miezin, F. M., Wenger, K. K., Kang, H. C., et al. (2006). A core system for the implementation of task sets. *Neuron*, *50*, 799–812. https://doi.org/10.1016/j.neuron.2006.04.031, PubMed: 16731517

Douchamps, V., Jeewajee, A., Blundell, P., Burgess, N., & Lever, C. (2013). Evidence for encoding versus retrieval scheduling in the hippocampus by theta phase and acetyl-choline. *Journal of Neuroscience*, *33*, 8689–8704. https://doi.org/10.1523/JNEUROSCI.4483-12.2013, PubMed: 23678113

Duncan, K. D., Sadanand, A., & Davachi, L. (2012). Memory's penumbra: Episodic memory decisions induce lingering mnemonic biases. *Science*, *337*, 485–487. https://doi.org/10.1126/science.1221936, PubMed: 22837528

Dunn, J. C. (1974). Well-separated clusters and optimal fuzzy partitions. *Journal of Cybernetics*, *4*, 95–104. https://doi.org/10.1080/01969727408546059

Fox, M. D., Snyder, A. Z., Vincent, J. L., Corbetta, M., Essen, D. C. V., & Raichle, M. E. (2005). The human brain is intrinsically organized into dynamic, anticorrelated functional networks. *Proceedings of the National Academy of Sciences of the U.S.A.*, *102*, 9673–9678. https://doi.org/10.1073/pnas.0504136102, PubMed: 15976020

González-García, C., & He, B. J. (2021). A gradient of sharpening effects by perceptual prior across the human cortical hierarchy. *Journal of Neuroscience*, *41*, 167–178. https://doi.org/10.1523/JNEUROSCI.2023-20.2020, PubMed: 33208472

Gratton, C., Neta, M., Sun, H., Ploran, E. J., Schlaggar, B. L., Wheeler, M. E., et al. (2016). Distinct stages of moment-to-moment processing in the cinguloopercular and frontoparietal networks. *Cerebral Cortex*, *27*, 2403–2417. https://doi.org/10.1093/cercor/bhw092, PubMed: 27095824

Hasselmo, M. E. (2005). What is the function of hippocampal theta rhythm?—Linking behavioral data to phasic properties of field potential and unit recording data. *Hippocampus*, *15*, 936–949. https://doi.org/10.1002/hipo.20116, PubMed: 16158423

Hasselmo, M. E. (2006). The role of acetylcholine in learning and memory. *Current Opinion in Neurobiology*, *16*, 710–715. https://doi.org/10.1016/j.conb.2006.09.002, PubMed: 17011181

Hasselmo, M. E., Bodelon, C., & Wyble, B. P. (2002). A proposed function for hippocampal theta rhythm: Separate phases of encoding and retrieval enhance reversal of prior learning. *Neural Computation*, *14*, 793–817. https://doi.org/10.1162/089976602317318965, PubMed: 11936962

Haufe, S., Meinecke, F., Görgen, K., Dähne, S., Haynes, J.-D., Blankertz, B., et al. (2014). On the interpretation of weight vectors of linear models in multivariate neuroimaging. *Neuroimage*, *87*, 96–110. https://doi.org/10.1016/j.neuroimage.2013.10.067, PubMed: 24239590

Higgins, C., Liu, Y., Vidaurre, D., Kurth-Nelson, Z., Dolan, R., Behrens, T. E. J., et al. (2021). Replay bursts in humans coincide with activation of the default mode and parietal alpha networks. *Neuron*, *109*, 882–893. https://doi.org/10.1016/j.neuron.2020.12.007, PubMed: 33357412

Kam, J. W. Y., Lin, J. J., Solbakk, A.-K., Endestad, T., Larsson, P. G., & Knight, R. T. (2019). Default network and frontoparietal control network theta connectivity supports internal attention. *Nature Human Behaviour*, *3*, 1263–1270. https://doi.org/10.1038/s41562-019-0717-0, PubMed: 31477910

Kay, K., & Frank, L. M. (2019). Three brain states in the hippocampus and cortex. *Hippocampus*, *29*, 184–238. https://doi.org/10.1002/hipo.22956

Kerrén, C., Linde-Domingo, J., Hanslmayr, S., & Wimber, M. (2018). An optimal oscillatory phase for pattern reactivation during memory retrieval. *Current Biology*, *28*, 3383–3392. https://doi.org/10.1016/j.cub.2018.08.065, PubMed: 30344116

Kerrén, C., van Bree, S., Griffiths, B. J., & Wimber, M. (2022). Phase separation of competing memories along the human hippocampal theta rhythm. *eLife*, *11*, e80633. https://doi.org/10.7554/eLife.80633, PubMed: 36394367

Khanna, A., Pascual-Leone, A., & Farzan, F. (2014). Reliability of resting-state microstate features in electroencephalography. *PLoS One*, *9*, e114163. https://doi.org/10.1371/journal.pone.0114163, PubMed: 25479614

Kim, H. (2010). Dissociating the roles of the default-mode, dorsal, and ventral networks in episodic memory retrieval. *Neuroimage*, *50*, 1648–1657. https://doi.org/10.1016/j.neuroimage.2010.01.051, PubMed: 20097295

Koenig, T., Prichep, L., Lehmann, D., Sosa, P., Braeker, E., Kleinlogel, H., et al. (2002). Millisecond by millisecond, year by year: Normative EEG microstates and developmental stages. *Neuroimage*, *16*, 41–48. https://doi.org/10.1006/nimg.2002.1070, PubMed: 11969316

Konkle, T., Brady, T. F., Alvarez, G. A., & Oliva, A. (2010). Conceptual distinctiveness supports detailed visual long-term memory for real-world objects. *Journal of Experimental Psychology: General*, *139*, 558–578. https://doi.org/10.1037/a0019165, PubMed: 20677899

Kragel, J. E., & Polyn, S. M. (2013). Functional interactions between large-scale networks during memory search. *Cerebral Cortex*, *25*, 667–679. https://doi.org/10.1093/cercor/bht258, PubMed: 24084128

Kuhl, B. A., Bainbridge, W. A., & Chun, M. M. (2012). Neural reactivation reveals mechanisms for updating memory. *Journal of Neuroscience*, *32*, 3453–3461. https://doi.org/10.1523/JNEUROSCI.5846-11.2012, PubMed: 22399768

Lehmann, D., Ozaki, H., & Pal, I. (1987). EEG alpha map series: Brain micro-states by space-oriented adaptive segmentation. *Electroencephalography and Clinical Neurophysiology*, *67*, 271–288. https://doi.org/10.1016/0013-4694(87)90025-3, PubMed: 2441961

Long, N. M., & Kuhl, B. A. (2019). Decoding the tradeoff between encoding and retrieval to predict memory for overlapping events. *Neuroimage*, *201*, 116001. https://doi.org/10.1016/j.neuroimage.2019.07.014, PubMed: 31299369

Long, N. M., & Kuhl, B. A. (2021). Cortical representations of visual stimuli shift locations with changes in memory states. *Current Biology*, *31*, 1119–1126. https://doi.org/10.1016/j.cub.2021.01.004, PubMed: 33577747

Long, N. M., Lee, H., & Kuhl, B. A. (2016). Hippocampal mismatch signals are modulated by the strength of neural predictions and their similarity to outcomes. *Journal of Neuroscience*, *36*, 12677–12687. https://doi.org/10.1523/JNEUROSCI.1850-16.2016, PubMed: 27821577

Meeter, M., Murre, J. M. J., & Talamini, L. M. (2004). Mode shifting between storage and recall based on novelty detection in oscillating hippocampal circuits. *Hippocampus*, *14*, 722–741. https://doi.org/10.1002/hipo.10214

Michel, C. M., & Koenig, T. (2018). EEG microstates as a tool for studying the temporal dynamics of whole-brain neuronal networks: A review. *Neuroimage*, *180*, 577–593. https://doi.org/10.1016/j.neuroimage.2017.11.062, PubMed: 29196270

Milligan, G. W. (1980). An examination of the effect of six types of error perturbation on fifteen clustering algorithms. *Psychometrika*, *45*, 325–342. https://doi.org/10.1007/BF02293907

Milligan, G. W. (1981). A Monte Carlo study of thirty internal criterion measures for cluster analysis. *Psychometrika*, *46*, 187–199. https://doi.org/10.1007/BF02293899

Milz, P., Faber, P., Lehmann, D., Koenig, T., Kochi, K., & Pascual-Marqui, R. (2016). The functional significance of EEG microstates—Associations with modalities of thinking. *Neuroimage*, *125*, 643–656. https://doi.org/10.1016/j.neuroimage.2015.08.023, PubMed: 26285079

Murphy, A. C., Bertolero, M. A., Papadopoulos, L., Lydon-Staley, D. M., & Bassett, D. S. (2020). Multimodal network dynamics underpinning working memory. *Nature Communications*, *11*, 3035. https://doi.org/10.1038/s41467-020-15541-0, PubMed: 32541774

Murray, M. M., Brunet, D., & Michel, C. M. (2008). Topographic ERP analyses: A step-by-step tutorial review. *Brain Topography*, *20*, 249–264. https://doi.org/10.1007/s10548-008-0054-5, PubMed: 18347966

Niu, Z., Jia, L., Liu, Y., Wang, Q., Li, Y., Yang, L., et al. (2022). Scale-free dynamics of microstate sequence in negative schizophrenia and depressive disorder. *Computers in Biology and Medicine*, *143*, 105287. https://doi.org/10.1016/j.compbiomed.2022.105287, PubMed: 35172224

Nolan, H., Whelan, R., & Reilly, R. (2010). FASTER: Fully Automated Statistical Thresholding for EEG artifact Rejection. *Journal of Neuroscience Methods*, *192*, 152–162. https://doi.org/10.1016/j.jneumeth.2010.07.015, PubMed: 20654646

Pascual-Marqui, R. D., Michel, C. M., & Lehmann, D. (1995). Segmentation of brain electrical activity into microstates: Model estimation and validation. *IEEE Transactions on Biomedical Engineering*, *42*, 658–665. https://doi.org/10.1109/10.391164, PubMed: 7622149

Patil, A., & Duncan, K. (2018). Lingering cognitive states shape fundamental mnemonic abilities. *Psychological Science*, *29*, 45–55. https://doi.org/10.1177/0956797617728592, PubMed: 29116882

Polyn, S. M., Natu, V. S., Cohen, J. D., & Norman, K. A. (2005). Category-specific cortical activity precedes retrieval during memory search. *Science*, *310*, 1963–1966. https://doi.org/10.1126/science.1117645, PubMed: 16373577

Poulsen, A. T., Pedroni, A., Langer, N., & Hansen, L. K. (2018). Microstate eeglab toolbox: An introductory guide. *BioRxiv 289860. March 27 2018 [cited June 6 2022.]* Available from: https://doi.org/10.1101/289850

Power, J. D., Cohen, A. L., Nelson, S. M., Wig, G. S., Barnes, K. A., Church, J. A., et al. (2011). Functional network organization of the human brain. *Neuron*, *72*, 665–678. https://doi.org/10.1016/j.neuron.2011.09.006, PubMed: 22099467

Preston, A. R., & Eichenbaum, H. (2013). Interplay of hippocampus and prefrontal cortex in memory. *Current Biology*, *23*, R764–R773. https://doi.org/10.1016/j.cub.2013.05.041, PubMed: 24028960

Raccah, O., Daitch, A. L., Kucyi, A., & Parvizi, J. (2018). Direct cortical recordings suggest temporal order of task-evoked responses in human dorsal attention and default networks. *Journal of Neuroscience*, *38*, 10305–10313. https://doi.org/10.1523/JNEUROSCI.0079-18.2018, PubMed: 30315126

Raichle, M. E., MacLeod, A. M., Snyder, A. Z., Powers, W. J., Gusnard, D. A., & Shulman, G. L. (2001). A default mode of brain function. *Proceedings of the National Academy of Sciences of the U.S.A.*, *98*, 676–682. https://doi.org/10.1073/pnas.98.2.676, PubMed: 11209064

Richter, F. R., Chanales, A. J., & Kuhl, B. A. (2016). Predicting the integration of overlapping memories by decoding mnemonic processing states during learning. *Neuroimage*, *124*, 323–335. https://doi.org/10.1016/j.neuroimage.2015.08.051, PubMed: 26327243

Ritchey, M., Wing, E. A., LaBar, K. S., & Cabeza, R. (2013). Neural similarity between encoding and retrieval is related to memory via hippocampal interactions. *Cerebral Cortex*, *23*, 2818–2828. https://doi.org/10.1093/cercor/bhs258, PubMed: 22967731

Rousseeuw, P. J. (1987). Silhouettes: A graphical aid to the interpretation and validation of cluster analysis. *Journal of Computational and Applied Mathematics*, *20*, 54–65. https://doi.org/10.1016/0377-0427(87)90125-7

Seitzman, B. A., Abell, M., Bartley, S. C., Erickson, M. A., Bolbecker, A. R., & Hetrick, W. P. (2017). Cognitive manipulation of brain electric microstates. *Neuroimage*, *146*, 533–543. https://doi.org/10.1016/j.neuroimage.2016.10.002, PubMed: 27742598

Skrandies, W. (1990). Global field power and topographic similarity. *Brain Topography*, *3*, 137–141. https://doi.org/10.1007/BF01128870, PubMed: 2094301

Smith, D. E., Moore, I. L., & Long, N. M. (2022). Temporal context modulates encoding and retrieval of overlapping events. *Journal of Neuroscience*, *42*, 3000–3010. https://doi.org/10.1523/JNEUROSCI.1091-21.2022

Tamano, R., Ogawa, T., Katagiri, A., Cai, C., Asai, T., & Kawanabe, M. (2022). Event-related microstate dynamics represents working memory performance. *Neuroimage*, 263. https://doi.org/10.1016/j.neuroimage.2022.119669, PubMed: 36206941

Tang, Y.-Y., Rothbart, M. K., & Posner, M. I. (2012). Neural correlates of establishing, maintaining, and switching brain states. *Trends in Cognitive Sciences*, *16*, 330–337. https://doi.org/10.1016/j.tics.2012.05.001, PubMed: 22613871

Tomescu, M. I., Papasteri, C., Sofonea, A., Boldasu, R., Kebets, V., Pistol, C. A. D., et al. (2022). Spontaneous thought and microstate activity modulation by social imitation. *Neuroimage*, *249*, 118878. https://doi.org/10.1016/j.neuroimage.2022.118878, PubMed: 34999201

Tzovara, A., Murray, M. M., Michel, C. M., & De Lucia, M. (2012). A tutorial review of electrical neuroimaging from group-average to single-trial event-related potentials. *Developmental Neuropsychology*, *37*, 518–544. https://doi.org/10.1080/87565641.2011.636851, PubMed: 22889343

van Kesteren, M. T., Ruiter, D. J., Fernández, G., & Henson, R. N. (2012). How schema and novelty augment memory formation. *Trends in Neurosciences*, *35*, 211–219. https://doi.org/10.1016/j.tins.2012.02.001, PubMed: 22398180

Wheeler, M. E., Petersen, S. E., & Buckner, R. L. (2000). Memory's echo: Vivid remembering reactivates sensory-specific cortex. *Proceedings of the National Academy of Sciences of the U.S.A.*, *97*, 11125–11129. https://doi.org/10.1073/pnas.97.20.11125, PubMed: 11005879

Yeo, B. T. T., Krienen, F. M., Sepulcre, J., Sabuncu, M. R., Lashkari, D., Hollinshead, M., et al. (2011). The organization of the human cerebral cortex estimated by intrinsic functional connectivity. *Journal of Neurophysiology*, *106*, 1125–1165. https://doi.org/10.1152/jn.00338.2011, PubMed: 21653723

Yuan, H., Zotev, V., Phillips, R., Drevets, W. C., & Bodurka, J. (2012). Spatiotemporal dynamics of the brain at rest—Exploring EEG microstates as electrophysiological signatures of bold resting state networks. *Neuroimage*, *60*, 2062–2072. https://doi.org/10.1016/j.neuroimage.2012.02.031, PubMed: 22381593

Zanesco, A. P. (2020). EEG electric field topography is stable during moments of high field strength. *Brain Topography*, *33*, 450–460. https://doi.org/10.1007/s10548-020-00780-7

Zanesco, A. P., Denkova, E., & Jha, A. P. (2021a). Associations between self-reported spontaneous thought and temporal sequences of EEG microstates. *Brain and Cognition*, *150*, 105696. https://doi.org/10.1016/j.bandc.2021.105696, PubMed: 33706148

Zanesco, A. P., Denkova, E., & Jha, A. P. (2021b). Self-reported mind wandering and response time variability differentiate prestimulus electroencephalogram microstate dynamics during a sustained attention task. *Journal of Cognitive Neuroscience*, *33*, 28–45. https://doi.org/10.1162/jocn_a_01636, PubMed: 33054554